True Cramer–Rao Bound for Timing Recovery From a Bandlimited Linearly Modulated Waveform With Unknown Carrier Phase and Frequency

Nele Noels, *Student Member, IEEE*, Henk Wymeersch, *Student Member, IEEE*, Heidi Steendam, *Member, IEEE*, and Marc Moeneclaey, *Fellow, IEEE*

***Abstract*—This paper derives the Cramer–Rao bound (CRB) related to the estimation of the time delay of a linearly modulated bandpass signal with unknown carrier phase and frequency. We consider the following two scenarios: joint estimation of the time delay, the carrier phase, and the carrier frequency; and joint estimation of the time delay and the carrier frequency irrespective of the carrier phase. The transmit pulse is a *bandlimited* square-root Nyquist pulse. For each scenario, the transmitted symbols constitute either an *a priori* known training sequence or an unknown random data sequence. In spite of the presence of random data symbols and/or a random carrier phase, we obtain a relatively simple expression of the CRB, from which the effect of the constellation and the transmit pulse are easily derived. We show that the penalty resulting from estimating the time delay irrespective of the carrier phase decreases with increasing observation interval. However, the penalty, caused by not knowing the data symbols *a priori*, cannot be reduced by increasing the observation interval. Comparison of the true CRB to existing symbol synchronizer performance reveals that decision-directed timing recovery is close to optimum for moderate-to-large signal-to-noise ratios.**

***Index Terms*—Carrier synchronization, Cramer–Rao bound (CRB), symbol synchronization, timing estimation.**

I. Introduction

THE Cramer–Rao bound (CRB) is a lower bound on the error variance of any unbiased estimate, and as such, serves as a useful benchmark for practical estimators [1]. In many cases, the statistics of the observation depend not only on the vector parameter to be estimated, but also on a *nuisance* vector parameter we do not want to estimate. A common example is the estimation of the synchronization parameters (carrier frequency offset, carrier phase, time delay) of a signal carrying digital information, with the unknown data symbols acting as nuisance parameters. The presence of the nuisance parameters makes the computation of the likelihood function and the corresponding CRB very hard.

In order to avoid the computational complexity caused by the nuisance parameters, a *modified* CRB (MCRB) has been derived in [2] and [3]. The MCRB is much simpler to evaluate than the *true* CRB, but is, in general, looser. In [4], the high signal-to-noise ratio (SNR) limit of the true CRB related to the estimation of a scalar parameter has been evaluated analytically. In [5], the low-SNR limits of the true CRBs for timing recovery, both irrespective of the carrier phase and with *a priori* known carrier phase, have been obtained analytically, assuming perfect carrier frequency recovery; the low-SNR limits of the true CRBs for carrier phase and frequency estimation, assuming perfect timing, are dealt with in [6]. The closed-form expression of the CRB in the presence of random data has been presented only for very few cases, pertaining either to carrier phase and frequency estimation, assuming the timing to be known [7]–[10], or to timing estimation, assuming perfect carrier synchronization [11].

However, in practice, it is unusual to perform carrier synchronization prior to timing recovery. Therefore, in this paper, we further consider the true CRB related to time-delay estimation in the following more realistic scenarios: joint estimation of the time delay, the carrier phase, and the carrier frequency; and joint estimation of the time delay and the carrier frequency irrespective of the carrier phase. The transmitted symbols are either known (training sequence) or unknown (random data) to the receiver, and are taken from an M-ary phase-shift keying (M-PSK), M-ary quadrature amplitude modulation (M-QAM), or M-ary pulse amplitude modulation (M-PAM) constellation. The transmit pulse is a bandlimited square-root Nyquist pulse. In Section II, the CRB is defined and some related results from the literature are briefly reviewed. We tackle the problem of drastically reducing the computational complexity of the CRB in Section III. Section IV investigates the behavior of the CRB as a function of the SNR, the constellation, the transmitted sequence length, and the shape of the transmit pulse. The CRB is compared with the actual performance of two timing synchronizers in Section V. In Section VI, conclusions are drawn and suggestions for further research formulated. One of the main conclusions is that for moderate and large observation intervals,

Paper approved by R. Reggiannini, the Editor for Synchronization and Wireless Applications of the IEEE Communications Society. Manuscript received December 20, 2001; revised July 22, 2002 and September 9, 2003. This work was supported by the Interuniversity Attraction Poles Program P5/11-Belgian State-Belgian Science Policy.

The authors are with the Telecommunications and Information Processing Department, Ghent University, B-9000 Gent, Belgium (e-mail: nnoels@telin.UGent.be; hwymeers@telin.UGent.be; hs@telin.UGent.be; mm@telin.UGent.be).

Digital Object Identifier 10.1109/TCOMM.2004.823648

the CRBs for timing estimation in the above two scenarios are essentially the same as with perfect carrier synchronization.

II. Problem Formulation

Let us consider the complex baseband representation $r(t)$ of a noisy linearly modulated signal

$$r(t)=\sum_{k=-K}^{K} a_k h(t-kT-\tau)\exp(j(\theta+2\pi Ft))+w(t) \quad (1)$$

where $\mathbf{a}=(a_{-K},\ldots,a_K)$ is a vector of $L=2K+1$ symbols taken from an M-PSK, M-QAM, or M-PAM constellation; $h(t)$ is a *real-valued* unit-energy square-root Nyquist pulse; τ is the time delay, θ is the carrier phase at $t=0$, F is the carrier frequency offset; T is the symbol interval; $w(t)$ is complex-valued zero-mean Gaussian noise with independent real and imaginary parts, each having a normalized power spectral density (PSD) of $N_0/(2E_s)$, with E_s and N_0 denoting the symbol energy and the noise PSD, respectively. The transmitted symbols are either unknown random data or *a priori* known training symbols. In the former case, the random data symbols are assumed to be statistically independent (hence, uncoded) and equally likely, satisfying the normalization constraint $E[|a_k|^2]=1$. In the latter case, the symbols of the training sequence are selected from the same normalized constellations.

Suppose that one is able to produce from an observation vector $\mathbf{r}$ an *unbiased* estimate $\hat{\mathbf{u}}$ of a deterministic vector parameter $\mathbf{u}$. Then the estimation error variance is lower bounded by the CRB [1]: $E_{\mathbf{r}}[(\hat{u}_i-u_i)^2]\geq \mathrm{CRB}_i(\mathbf{u})$, where $\mathrm{CRB}_i(\mathbf{u})$ is the ith diagonal element of the inverse of the *Fisher information matrix* (FIM) $\mathbf{J}(\mathbf{u})$. The (i,j)th element of $\mathbf{J}(\mathbf{u})$ is given by

$$\begin{aligned}\mathbf{J}_{i,j}&=E_{\mathbf{r}}\left[-\frac{\partial^2}{\partial u_i\partial u_j}\ln(p(\mathbf{r};\mathbf{u}))\right]\\&=E_{\mathbf{r}}\left[\frac{\partial}{\partial u_i}\ln(p(\mathbf{r};\mathbf{u}))\frac{\partial}{\partial u_j}\ln(p(\mathbf{r};\mathbf{u}))\right].\end{aligned} \quad (2)$$

Note that $\mathbf{J}(\mathbf{u})$ is a symmetrical matrix. When the element $\mathbf{J}_{ij}(\mathbf{u})=0$, the parameters u_i and u_j are said to be *decoupled*. The probability density $p(\mathbf{r};\mathbf{u})$ of $\mathbf{r}$, viewed as a function of $\mathbf{u}$, is called the *likelihood function* of $\mathbf{u}$, while $\ln(p(\mathbf{r};\mathbf{u}))$ is the *log-likelihood function (LLF)* of $\mathbf{u}$. The expectation $E_r[\cdot]$ in (2) is with respect to $p(\mathbf{r};\mathbf{u})$.

When the observation $\mathbf{r}$ depends not only on the parameter $\mathbf{u}$ to be estimated, but also on a nuisance vector parameter $\mathbf{v}$, the likelihood function of $\mathbf{u}$ is obtained by averaging the likelihood function $p(\mathbf{r}\,|\,\mathbf{v};\mathbf{u})$ of the vector $(\mathbf{u},\mathbf{v})$ over the *a priori* distribution of the nuisance parameter: $p(\mathbf{r};\mathbf{u})=E_{\mathbf{v}}[p(\mathbf{r}\,|\,\mathbf{v};\mathbf{u})]$. We refer to $p(\mathbf{r}\,|\,\mathbf{v};\mathbf{u})$ as the *joint* likelihood function, as $p(\mathbf{r}\,|\,\mathbf{v};\mathbf{u})$ is relevant to the joint estimation of $\mathbf{u}$ and $\mathbf{v}$.

We investigate two scenarios. For each scenario, the transmitted symbols form either a known training sequence or an unknown random data sequence.

Scenario (i): joint estimation of (τ,F,θ). The useful parameter is given by $\mathbf{u}=(\tau,F,\theta)$. There is no nuisance parameter when the transmitted symbols are known. In the case of random data, the nuisance parameter is given by $\mathbf{v}=\mathbf{a}$.

Scenario (ii): joint estimation of $(\tau,\mathbf{F})$ irrespective of θ. The useful parameter is given by $\mathbf{u}=(\tau,F)$. The nuisance parameter is given by $\mathbf{v}=\theta$ when the transmitted symbols are known, or by $\mathbf{v}=(\theta,\mathbf{a})$ when the symbols are random data. In this scenario, θ is considered as uniformly distributed in $(-\pi,\pi)$.

For both scenarios, the joint likelihood function $p(\mathbf{r}\,|\,\mathbf{v};\mathbf{u})$ is, within a factor not depending on $(\mathbf{u},\mathbf{v})$, given by

$$p(\mathbf{r}\,|\,\mathbf{v};\mathbf{u})=\prod_{k=-K}^{K}F(a_k,\tilde{x}_k) \quad (3)$$

where

$$F(a_k,\tilde{x}_k)=\exp\left(\frac{E_s}{N_0}(2\Re[a_k^*\tilde{x}_k]-|a_k|^2)\right). \quad (4)$$

In (3), $\mathbf{r}$ is a vector representation of the signal $r(t)$ from (1), and $\tilde{x}_k=x_k e^{-j\theta}$, where x_k is defined as

$$x_k=\int e^{-j2\pi Ft}r(t)h(t-kT-\tau)\,dt. \quad (5)$$

Note that $\tilde{x}_k$ is obtained by first frequency-correcting $r(t)$ by an amount $-F$, then applying the result to a filter that is matched to the transmit pulse $h(t)$, sampling the matched-filter output at instant $kT+\tau$, and finally rotating the matched-filter output sample over an angle $-\theta$. Hence, $\tilde{x}_k$ is a function of (τ,F,θ), whereas x_k depends only on (τ,F). The LLF $\ln(p(\mathbf{r};\mathbf{u}))$ resulting from (3) is

$$\ln p(\mathbf{r};\mathbf{u})=\ln\left(E_{\mathbf{v}}\left[\prod_{k=-K}^{K}F(a_k,\tilde{x}_k)\right]\right). \quad (6)$$

Computation of the CRB requires the substitution of (6) into (2), and the evaluation of the various expectations included in (6) and (2).

As the evaluation of the expectations involved in $\mathbf{J}(\mathbf{u})$ and $p(\mathbf{r};\mathbf{u})$ is quite tedious, a simpler lower bound, called the modified CRB (MCRB), has been derived in [2] and [3], i.e., $E_{\mathbf{r}}[(\hat{u}_i-u_i)^2]\geq \mathrm{CRB}_i(\mathbf{u})\geq \mathrm{MCRB}_i(\mathbf{u})$, where $\mathrm{MCRB}_i(\mathbf{u})$ is the ith diagonal element of the inverse of the *modified* Fisher information matrix (MFIM) $\mathbf{J}_M(\mathbf{u})$. The (i,j)th element of $\mathbf{J}_M(\mathbf{u})$ is given by

$$\begin{aligned}(\mathbf{J}_M(\mathbf{u}))_{ij}&=E_{\mathbf{r},\mathbf{v}}\left[-\frac{\partial^2}{\partial u_i\partial u_j}\ln(p(\mathbf{r}|\mathbf{v};\mathbf{u}))\right]\\&=E_{\mathbf{r},\mathbf{v}}\left[\frac{\partial}{\partial u_i}\ln(p(\mathbf{r}|\mathbf{v};\mathbf{u}))\frac{\partial}{\partial u_j}\ln(p(\mathbf{r}|\mathbf{v};\mathbf{u}))\right]\end{aligned} \quad (7)$$

and $E_{r,v}[\cdot]$ denotes averaging over both $\mathbf{r}$ and $\mathbf{v}$, i.e., with respect to $p(\mathbf{r},\mathbf{v};\mathbf{u})$. Note that (7) is much simpler than (2) as far as analytical evaluation is concerned.

Let us introduce the Nyquist pulse $g(t)$ given by

$$g(t)=\int_{-\infty}^{+\infty}h(v)h(t+v)\,dv \quad (8)$$

and denote its first and second derivate with respect to t as $\dot{g}(t)$ and $\ddot{g}(t)$, respectively; for real-valued $h(t)$, the pulses $g(t)$ and $\ddot{g}(t)$ are even in t, whereas $\dot{g}(t)$ is an odd function of t. Then,

assuming *random data*, the MCRB for timing estimation, corresponding to $r(t)$ from (1), is for both scenarios (i) and (ii) given by [2], [3]

$$E[(\hat{\tau}-\tau)^2/T^2] \geq \mathrm{MCRB} = \frac{1}{2\frac{E_s}{N_0}LC_1} \tag{9}$$

where

$$C_1 = -\ddot{g}(0)T^2 = T^2\int (\dot{h}(t))^2\,dt \tag{10}$$

and $L = 2K+1$ denotes the number of symbols transmitted within the observation interval. Note that in (9), the timing error has been normalized by the symbol interval T. The MCRB is inversely proportional to L and to E_s/N_0, and does not depend on the symbol constellation; the shape of the transmit pulse $h(t)$ affects only C_1, which is an increasing function of the excess bandwidth of the transmit pulse $h(t)$.

When L *known symbols* are transmitted, the MCRB depends on the particular training sequence selected. We consider a training sequence such that, as L grows, the time averages of interest, involving the particular sequence, converge to the corresponding statistical averages of a sequence of random data symbols that belong to the same constellation as the training symbols. It will be assumed that the sequence length is sufficiently large, so that the MFIM converges to the MFIM that corresponds to random data; hence, the MCRB for known symbols converges to the MCRB (9) for random data. This is illustrated in Appendix 1. In the case of known symbols, not only the MCRB, but also the CRB, depends on the particular training sequence selected. Again, it will be assumed that the sequence length is sufficiently large, so that, using similar arguments as above, the dependence of the CRB on the training sequence can safely be ignored.

Let us define by ACRB_∞ and ACRB_0 the high-SNR and low-SNR asymptotic CRBs (ACRBs) that are obtained as the limit of CRB for $E_s/N_0 \to \infty$ and $E_s/N_0 \to 0$, respectively. In [4], the high-SNR limit of the CRB related to the estimation of a *scalar* parameter has been evaluated analytically. For timing estimation when both the carrier phase and frequency are known [which we will show to be relevant to Scenario (i)], it follows from [4] that ACRB_∞ equals MCRB from (9) when the data symbols are random; in the case of a training sequence, ACRB_∞ converges to MCRB with increasing sequence length L. For timing estimation, irrespective of the carrier phase and assuming the carrier frequency to be known [which we will show to be relevant to Scenario (ii)], it follows from [4] that ACRB_∞, for random data symbols as well as *a priori* known training symbols, converges to MCRB from (9) when the sequence length increases. Also, a closed-form expression can be derived for the low-SNR limit ACRB_0. In [5], this has been accomplished assuming random data symbols. One obtains

$$\mathrm{ACRB}_0^{(\mathrm{i}),\mathrm{ra}} = \begin{cases} \mathrm{ACRB}_0^{(\mathrm{ii}),\mathrm{ra}}, \mathrm{M-PSK}(M>2), \mathrm{QAM} \\ \frac{1}{2}\mathrm{ACRB}_0^{(\mathrm{ii}),\mathrm{ra}}, \mathrm{PAM} \end{cases} \tag{11}$$

$$\mathrm{ACRB}_0^{(\mathrm{ii}),\mathrm{ra}} = \frac{1}{2L\left(\frac{E_s}{N_0}\right)^2(C_1-C_2)}, \mathrm{PSK}, \mathrm{QAM}, \mathrm{PAM}. \tag{12}$$

The two superscripts in (11)–(12) and in subsequent equations related to the CRBs refer to Scenario (i) or (ii) and to the receiver's knowledge about the transmitted symbols (ra: random data, kn: known training sequence). In (12), the quantity C_2 is given by

$$C_2 = \frac{1}{L}\sum_{k_1,k_2=-K}^{K} \dot{g}^2(k_1T-k_2T)T^2 \approx \sum_{n=-\infty}^{\infty}\dot{g}^2(nT)T^2 \tag{13}$$

The approximation in (13) is valid when the observation interval LT is much longer than the duration of $\dot{g}(t)$, in which case C_2 becomes independent of L. Equations (11)–(12) show that the ACRB_0 is inversely proportional to L (assuming large L, so that the approximation in (13) holds) and to the square of E_s/N_0. For a given constellation type, the number (M) of constellation points has no influence on ACRB_0. The shape of the transmit pulse $h(t)$ only affects (C_1-C_2), which grows (more rapidly than C_1) with the excess bandwidth of the transmit pulse $h(t)$. It should be noted that the ACRB_0 does not necessarily provide a *lower* bound on the actual timing error variance for moderate and large SNR. For complex-valued constellations (M-PSK with $M > 2$, M-QAM) both scenarios yield the same low-SNR limit of the CRB, whereas for real-valued constellations (M-PAM), Scenario (ii) yields an ACRB_0 that is twice as large as the ACRB_0 from Scenario (i). In the case where the transmitted symbols are known, the first scenario contains no nuisance parameters, so that the CRB and the MCRB coincide; hence, assuming a long training sequence, the corresponding CRB equals MCRB from (9). For the second scenario, the low-SNR limit ACRB_0 can be derived as in [5]; the result for a long training sequence is

$$\mathrm{ACRB}_0^{(\mathrm{ii}),\mathrm{kn}} = \frac{1}{2\left(\frac{E_s}{N_0}\right)^2L^2C_1} \tag{14}$$

which is proportional to $(E_s/N_0)^{-2}$ and L^{-2} (not L^{-1}).

III. Evaluation of the True CRB

In this section, we compute the true CRBs resulting from the two scenarios mentioned above, for both random data and known training symbols, assuming PAM, PSK, and QAM constellations, and a bandlimited square-root Nyquist pulse $h(t)$. We define $\mathbf{u}^T = (u_1,u_2,u_3) = (\tau, F, \theta)$.

A. Joint Estimation of τ, F and θ; Random Data Symbols

We first concentrate on rotationally symmetric constellations with $E[a^2(k)] = 0$, i.e., M-PSK with $M > 2$ and M-QAM, but not M-PAM. The case of M-PAM is dealt with at the end of this subsection.

Taking in (6) $\mathbf{v} = \mathbf{a}$, we obtain

$$\ln(p(\mathbf{r};\tau,\theta,F)) = \sum_{k=-K}^{K}\ln(I(\tilde{x}_k)) \tag{15}$$

where

$$I(\tilde{x}_k) = \sum_{i=0}^{M-1} F(\alpha_i,\tilde{x}_k) \tag{16}$$

$F(\alpha_i, \tilde{x}_k)$ is given by (4), and $\{\alpha_0, \alpha_1, \ldots, \alpha_{M-1}\}$ is the set of constellation points. Differentiation of (15) yields

$$\frac{\partial}{\partial u_\ell} \ln p(\mathbf{r}; \tau, \theta, F) = \frac{E_s}{N_0} \sum_{k=-K}^{K} \sum_{i=0}^{M-1} H(\alpha_i, \tilde{x}_k, \tilde{x}_{\ell,k}) \quad (17)$$

where

$$H(\alpha_i, \tilde{x}_k, \tilde{x}_{\ell,k}) = G(\alpha_i, \tilde{x}_k) 2\Re(\alpha_i^* \tilde{x}_{\ell,k}) \quad (18)$$

$$G(\alpha_i, \tilde{x}_k) = \frac{F(\alpha_i, \tilde{x}_k)}{I(\tilde{x}_k)} \quad (19)$$

and the subscript ℓ denotes differentiation with respect to u_ℓ, i.e.,

$$\tilde{x}_{l,k} = \frac{\partial}{\partial u_\ell}(\tilde{x}_k) \quad (20)$$

with $(u_1, u_2, u_3) = (\tau, F, \theta)$. Further, we define $x_{l,k}$ as $x_{l,k} = \tilde{x}_{l,k} e^{j\theta}$. Note that $x_{l,k}$ does not depend on θ; we have $x_{3,k} = -jx_k$ and $x_{l,k} = (\partial)/(\partial u_\ell)(x_k)$ for $\ell = 1, 2$. Taking (17) into account, $J_{\ell\ell'}$ from (2) can be represented as

$$J_{\ell\ell'} = \left(\frac{E_s}{N_0}\right)^2 \sum_{k_1,k_2=-K}^{K} \sum_{i_1,i_2=0}^{M-1} E\left[H\left(\alpha_{i_1}, \tilde{x}_{k_1}, \tilde{x}_{\ell,k_1}\right) \times H\left(\alpha_{i_2}, \tilde{x}_{k_2}, \tilde{x}_{\ell',k_2}\right)\right] \quad (21)$$

where $E[\cdot]$ denotes averaging over the quantities $\tilde{x}_{k_1}, \tilde{x}_{k_2}, \tilde{x}_{\ell,k_1}$, and $\tilde{x}_{\ell',k_2}$. As this averaging cannot be done analytically, we have to resort to a numerical evaluation. However, because of the correlation between the quantities $\tilde{x}_{k_1}, \tilde{x}_{k_2}, \tilde{x}_{\ell,k_1}$, and $\tilde{x}_{\ell',k_2}$, a brute-force numerical averaging is quite time consuming (brute force computation is briefly discussed in Section IV). Taking into account the Gaussian nature of the noise components in $\tilde{x}_k$ and $\tilde{x}_{\ell,k}$, we were able to perform *analytically* the averaging in (21) over $\tilde{x}_{\ell,k_1}$ and $\tilde{x}_{\ell',k_2}$, conditioned on $\tilde{x}_{k_1}$ and $\tilde{x}_{k_2}$. Further evaluation of (21) then requires *numerically* averaging only over $\tilde{x}_{k_1}$ and $\tilde{x}_{k_2}$, which are statistically independent. This procedure reduces the numerical complexity considerably. More details are outlined in [11] for the special case where F and θ are *a priori* known.

We obtain $J_{1,2} = 0$ and $J_{1,3} = 0$, which indicates that there is no coupling between the parameters τ and (θ, F). This means that (at least for small errors) the inaccuracy in carrier recovery does not impact timing delay estimation and vice versa. Consequently, the $\mathrm{CRB}^{(\mathrm{i}),\mathrm{ra}}$ is the same as the CRB from [11], which is related to timing recovery, assuming the carrier phase and frequency *a priori* known. This implies that the high and low SNR limits of the CRB are given by (9) and (11), respectively, and that the true CRB for M-PSK $(M > 2)$ and M-QAM is given by $1/J_{1,1}$

$$\frac{1}{\mathrm{CRB}^{(\mathrm{i}),\mathrm{ra}}} = 2L\frac{E_s}{N_0} C_1 A\left(\frac{E_s}{N_0}, M\right) - 2L\left(\frac{E_s}{N_0}\right)^2 \times C_2 B\left(\frac{E_s}{N_0}, M\right), \ \mathrm{M{-}PSK}(M > 2), \mathrm{QAM} \quad (22)$$

where

$$A\left(\frac{E_s}{N_0}, M\right) = E\left[\left|\sum_{i=0}^{M-1} G(\alpha_i, \tilde{x}_k)\alpha_i^*\right|^2\right] \quad (23)$$

$$B\left(\frac{E_s}{N_0}, M\right) = \left(E\left[\sum_{i=0}^{M-1} G(\alpha_i, \tilde{x}_k)\alpha_i^* \tilde{x}_k\right]\right)^2 - A\left(\frac{E_s}{N_0}, M\right). \quad (24)$$

The expectations in (23) and (24) are with respect to $\tilde{x}_k = a_k + N(k)$, where a_k is a data symbol taken randomly from the constellation, and $N(k)$ is a complex-valued zero-mean Gaussian random variable with uncorrelated real and imaginary parts, each having a variance equal to $N_0/2E_s$. The quantities $A(E_s/N_0, M)$, and $B(E_s/N_0, M)$ depend on E_s/N_0 and on the constellation, but *not* on the shape of the square-root Nyquist transmit pulse. The quantities $A(E_s/N_0, M)$ and $B(E_s/N_0, M)$ can easily be evaluated by means of numerically averaging. The shape of the transmit pulse affects only the quantities C_1 and C_2 in (22). Note that (F, θ) and τ being decoupled also implies that the CRBs for joint frequency and phase estimation under Scenario (i) with random data are the same as for joint carrier frequency and phase recovery, assuming the timing to be known; these CRBs related to carrier synchronization have been considered in [7]–[10].

Until now we have excluded from consideration the M-PAM constellation. The case of M-PAM can be dealt with in a similar way as above. It turns out that the CRB for M-PAM is related to the CRB for M^2-QAM by

$$\mathrm{CRB}^{(\mathrm{i}),\mathrm{ra}}_{\mathrm{M-PAM}}\left(\frac{E_s}{N_0}\right) = 2\mathrm{CRB}^{(\mathrm{i}),\mathrm{ra}}_{M^2-\mathrm{QAM}}\left(\frac{2E_s}{N_0}\right)$$
$$\mathrm{CRB}^{(\mathrm{i}),\mathrm{ra}}_{M^2-\mathrm{QAM}}\left(\frac{E_s}{N_0}\right) = \frac{1}{2}\mathrm{CRB}^{(\mathrm{i}),\mathrm{ra}}_{\mathrm{M-PAM}}\left(\frac{E_s}{2N_0}\right). \quad (25)$$

B. Joint Estimation of τ, F and θ; Known Training Symbols

In this scenario, there are no nuisance parameters. Hence, the CRB equals the MCRB, which, in principle, depends on the particular training sequence transmitted. For long training sequences, the elements $J_{1,2}$ and $J_{1,3}$ of the FIM (2) approach zero, whereas $J_{1,1}$ approaches 1/MCRB. Hence, also (θ, F) and τ are essentially decoupled, and the resulting CRB for timing estimation reduces to the MCRB given by (9).

C. Joint Estimation of τ and F Irrespective of θ; Random Data Symbols

Again, we first consider M-PSK with $M > 2$ and M-QAM, and deal with M-PAM at the end of this subsection. Taking in (6) $\mathbf{v} = (\mathbf{a}, \theta)$, the LLF $\ln(p(\mathbf{r}; \tau, F))$ is, within an arbitrary constant, given by

$$\ln(p(\mathbf{r}; \tau, F)) = \ln\left(\int_{-\pi}^{\pi} K(\theta, \mathbf{x}) d\theta\right) \quad (26)$$

where $\mathbf{x} = (x_{-K}, \ldots, x_K)$, and

$$K(\theta, \mathbf{x}) = \prod_{k=-K}^{K} I(x_k e^{-j\theta}). \quad (27)$$

The quantity $I(x_k e^{-j\theta})$ is given by (16), and $\{\alpha_0, \alpha_1, \alpha_{M-1}\}$ is the set of constellation points. Differentiation of (26) yields, for $\ell = 1, 2$

$$\frac{\partial}{\partial u_\ell} \ln p(r; \tau, F) = \frac{E_s}{N_0} \int_{-\pi}^{\pi} \sum_{k=-K}^{K} \sum_{i=0}^{M-1} M(\theta, \mathbf{x}) \times H(\alpha_i, x_k e^{-j\theta}, x_{\ell,k} e^{-j\theta})\, d\theta \quad (28)$$

where

$$M(\theta, \mathbf{x}) = \frac{K(\theta, \mathbf{x})}{\int_{-\pi}^{\pi} K(\theta, \mathbf{x})\, d\theta}. \quad (29)$$

Taking (28) into account, we derive from (2) the equation shown at the bottom of the page, where $E[\,\cdot\,]$ denotes averaging over the quantities $(\mathbf{x}, x_{\ell,k_1}, x_{\ell',k_2})$. Exploiting the Gaussian nature of the noise components, the average $E[\,\cdot\,]$ in (30) is computed by first *analytically* taking the expectation over x_{ℓ,k_1} and x_{ℓ',k_2}, conditioned on $\mathbf{x}$, and then *numerically* averaging over $\mathbf{x}$.

We obtain $J_{1,2} = 0$, which indicates that also in this scenario there is no coupling between the parameters τ and F. Consequently, the $\mathrm{CRB}^{(\mathrm{ii}),\mathrm{ra}}$ is the same as the CRB related to timing estimation irrespective of the carrier phase, assuming the carrier frequency to be known. This implies that the high and low SNR limits of this CRB are given by (9) and (12), respectively. Hence, $\mathrm{CRB} = 1/J_{1,1}$, yielding

$$\frac{1}{\mathrm{CRB}^{(\mathrm{ii}),\mathrm{ra}}} = 2\left(\frac{E_s}{N_0}\right)^2 L C_2 C\left(\frac{E_s}{N_0}, M, L\right) + 2\left(\frac{E_s}{N_0}\right) L(C_1 - C_2) D\left(\frac{E_s}{N_0}, M, L\right) \quad (31)$$

where

$$C\left(\frac{E_s}{N_0}, M, L\right) = E\begin{bmatrix} 2\Re^2(N(k,\mathbf{x})x_m) \\ -\Re(N(k,\mathbf{x})x_k N(m,\mathbf{x})x_m) \end{bmatrix} \quad (32)$$

$$D\left(\frac{E_s}{N_0}, M, L\right) = E[|N(k,\mathbf{x})|^2] \quad (33)$$

$$N(k,\mathbf{x}) = \int_{-\pi}^{\pi} \sum_{i=0}^{M-1} M(\theta,\mathbf{x}) G(\alpha_i, x_k e^{-j\theta}) \alpha_i^* e^{-j\theta} d\theta. \quad (34)$$

The expectations in (32) and (33) are with respect to $\mathbf{x} = \mathbf{a} + \mathbf{N}$, where $\mathbf{a}$ denotes the random data sequence, and $\mathbf{N}$ is a sequence of independent zero-mean complex-valued Gaussian random variables, with uncorrelated real and imaginary parts, each having a variance equal to $N_0/2E_s$. In (32), k and m represent two different integers from the interval $(-K, K)$. As in Scenario (i), the pulse shape affects the quantities C_1 and C_2, but not the numerical averages. Note that F and τ being decoupled implies that the CRB for frequency estimation under Scenario (ii) is the same as the CRB related to frequency recovery irrespective of the carrier phase, assuming the timing to be known; this CRB for frequency estimation has been considered in [9] and [10].

The case of M-PAM can be handled in a similar way as above. The CRB for M-PAM is given by (31), provided we replace in (31) the quantity $C(E_s/N_0, M, L)$ by

$$C_{\mathrm{PAM}}\left(\frac{E_s}{N_0}, M, L\right) = 2E\begin{bmatrix} \Re^2(N(k,\mathbf{x})x_m) \\ -\Re(N(k,\mathbf{x})x_k)\Re(N(m,\mathbf{x})x_m) \end{bmatrix}. \quad (35)$$

D. Joint Estimation of F and τ Irrespective of θ; Known Training Symbols

When the transmitted symbols are known at the receiver, the nuisance parameter is given by $\mathbf{v} = \theta$, and no averaging of the joint likelihood function (3) over the symbol sequence is required. Equation (28) remains valid, provided we remove all the summations over the constellation points, and replace α_i by the actual symbol a_k. For long training sequences, $J_{1,2}$ is essentially zero, meaning that F and τ are decoupled; hence, $\mathrm{CRB} = 1/J_{1,1}$, yielding

$$\frac{1}{\mathrm{CRB}^{(\mathrm{ii}),\mathrm{kn}}} = 2L\frac{E_s}{N_0} C_1 \times E\left[\left|\frac{\int_{-\pi}^{\pi} \cos\theta \exp\left(\frac{2E_sL}{N_0}|1+N|\cos\theta\right) d\theta}{\int_{-\pi}^{\pi} \exp\left(\frac{2E_sL}{N_0}|1+N|\cos\theta\right) d\theta}\right|^2\right] \quad (36)$$

where N is a zero-mean complex Gaussian random variable with uncorrelated real and imaginary parts, each having a variance equal to $N_0/(2E_sL)$. Note that the ratio $\mathrm{CRB}^{(\mathrm{ii}),\mathrm{kn}}/\mathrm{MCRB}$ is a function of E_sL/N_0 that is independent of the shape of the transmit pulse.

IV. Numerical Results and Discussion

As no further analytical simplification of (22), (31), and (36) seems possible, we have to resort to numerical computation. For Scenario (ii), the average with respect to θ [in (34) and (36)] is evaluated through numerical integration. Monte Carlo simulation techniques are used to evaluate the statistical expectations in (23)–(24), (32)–(33), (35), and (36) over the noise (and over the unknown data symbols) at each SNR. Note that these averages are independent of the transmit pulse, and are with respect to either a scalar [in (23)–(24) and (36)], or an L-dimensional vector [in (32)–(33) and (35)] with statistically indepen-

$$J_{\ell,\ell'} = \left(\frac{E_s}{N_0}\right)^2 \cdot \int_{\theta_1,\theta_2} \sum_{k_1,k_2=-K}^{K} \sum_{i_1,i_2=0}^{M-1} E\begin{bmatrix} M(\theta_1,\mathbf{x}) \\ \cdot H\left(\alpha_{i_1}, x_{k_1} e^{-j\theta_1}, x_{\ell,k_1} e^{-j\theta_1}\right) \\ \cdot M(\theta_2,\mathbf{x}) \\ \cdot H\left(\alpha_{i_2}, x_{k_2} e^{-j\theta_2}, x_{\ell',k_2} e^{-j\theta_2}\right) \end{bmatrix} d\theta_1 d\theta_2 \quad (30)$$

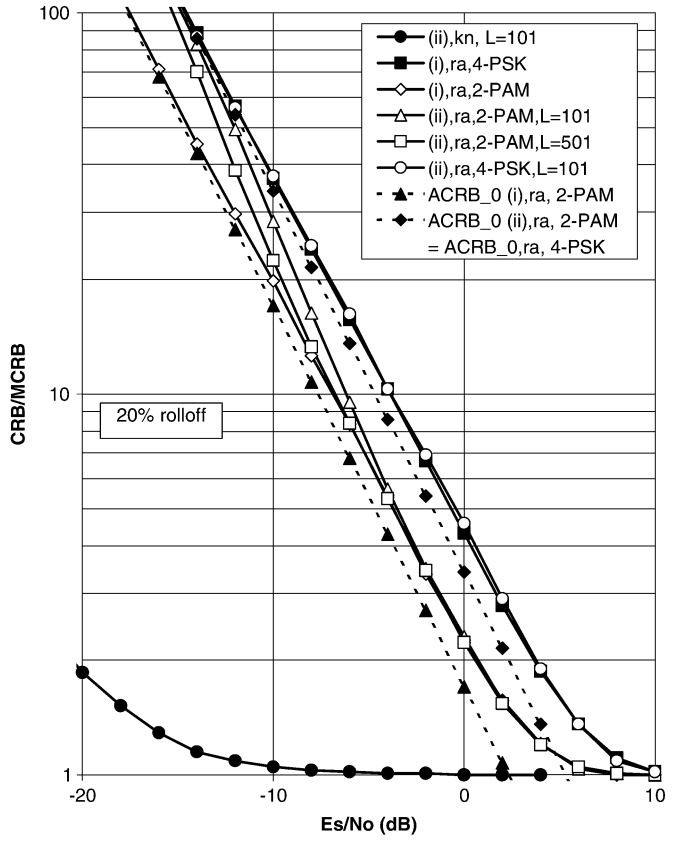

Fig. 1. CRB/MCRB for timing estimation [(i): Scenario (i); (ii): Scenario (ii); ra: random data sequence; kn: known training sequence] from a noisy linearly modulated signal characterized by a cosine 20% rolloff pulse; based on an observation of L symbol periods.

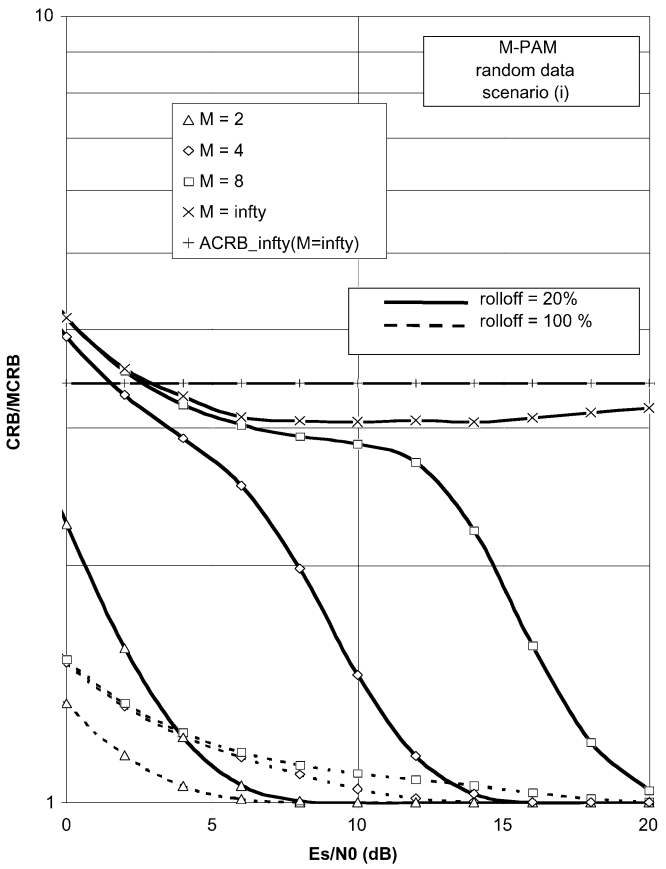

Fig. 2. CRB/MCRB for timing estimation from a noisy linearly modulated signal characterized by a cosine rolloff pulse and random M-PAM symbols.

dent components. This is in contrast to a brute-force evaluation that requires a numerical averaging over two correlated L-dimensional vectors $\{x_k\}$ and $\{x_{1,k}\}$ (and, for Scenario (ii), also one single and one double numerical integration over the carrier phase) in order to obtain $J_{1,1}$ [see (21) and (30)]; moreover, these brute-force computation results cannot be reused for a different shape of the transmit pulse.

In Fig. 1, we compare the CRBs resulting from the various scenarios, assuming 2-PAM and 4-PSK constellations; the transmit pulse is a square-root cosine rolloff pulse with a 20% excess bandwidth. The considered range of E_s/N_0 contains extremely low values, for the purpose of illustrating that the numerically computed CRBs are consistent with their analytically obtained low SNR limits. In the case of known symbols, the CRB for timing recovery, resulting from the joint estimation of τ, F, and θ, equals the MCRB from (9). Hence, for any other scenario, the ratio CRB/MCRB is a measure of the penalty caused by not knowing the transmitted symbols and/or not estimating θ jointly with (τ, F). The following observations can be made from Fig. 1.

For small (large) SNR, the CRBs converge to their corresponding ACRB_0 (to the MCRB (9)); the ACRB_0 for Scenario (ii) with known training symbols is not shown, because it falls outside the range displayed.

Of the two scenarios considered, Scenario (ii) yields the larger CRB. This indicates that estimating (τ, F) jointly with θ is potentially more accurate than estimating (τ, F) irrespective of θ. Indeed, as (τ, F), and θ are uncoupled, the joint estimation of (τ, F, θ) yields the same CRB as estimating (τ, F) when θ is *a priori* known, and this CRB is smaller than the one resulting from estimating (τ, F) irrespective of θ.

In the case of random data, $\mathrm{CRB}^{(\mathrm{i}),\mathrm{ra}}/\mathrm{MCRB}$ does not depend on L [see (9) and (22)]. This indicates that increasing the sequence length L cannot reduce the penalty caused by not knowing the transmitted symbols. The ratio $\mathrm{CRB}^{(\mathrm{ii}),\mathrm{ra}}/\mathrm{MCRB}$, on the contrary, does depend on L [see (9) and (31)]. Fig. 1 indicates that for a given $E_s/N_0, \mathrm{CRB}^{(\mathrm{ii}),\mathrm{ra}}/\mathrm{MCRB}$ converges to $\mathrm{CRB}^{(\mathrm{i}),\mathrm{ra}}/\mathrm{MCRB}$ when L increases. Hence, the penalty caused by estimating (τ, F) independently of θ is reduced by increasing L. For $L = 101$, this penalty is extremely small when E_s/N_0 exceeds about -4 dB in the case of 2-PAM, and for the whole range of E_s/N_0 in the case of 4-PSK.

When transmitting a long training sequence, $\mathrm{CRB}^{(\mathrm{ii}),\mathrm{kn}}/\mathrm{MCRB}$ only depends on E_sL/N_0 [see (9) and (36)]; hence, increasing the observation interval from L_1 to L_2 shifts the curve of $\mathrm{CRB}^{(\mathrm{ii}),\mathrm{kn}}/\mathrm{MCRB}$ to the left by $10\log(L_2/L_1)$ dB, so that the value of E_s/N_0 at which $\mathrm{CRB}^{(\mathrm{ii}),\mathrm{kn}}$ comes close to the MCRB is shifted by the same amount. We observe from Fig. 1 that for a moderate observation interval, $(L = 101)$ $\mathrm{CRB}^{(\mathrm{ii}),\mathrm{kn}}/\mathrm{MCRB}$ is essentially equal to one when E_s/N_0 exceeds about -4 dB. Hence, in the case of known symbols, the penalty resulting from estimating (τ, F) independently of θ can be safely ignored. Note from (36) that

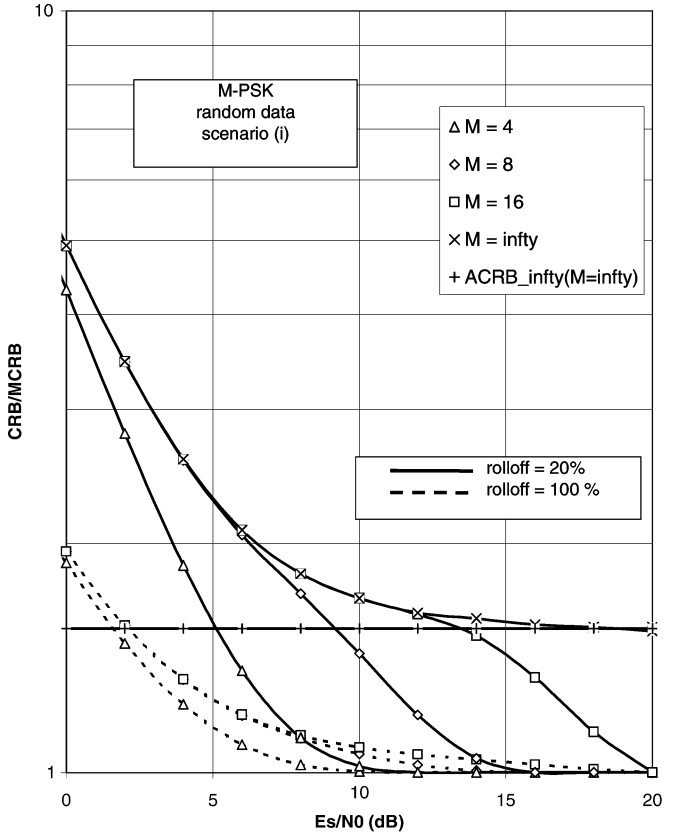

Fig. 3. CRB/MCRB for timing estimation from a noisy linearly modulated signal characterized by a cosine rolloff pulse and random M-PSK symbols.

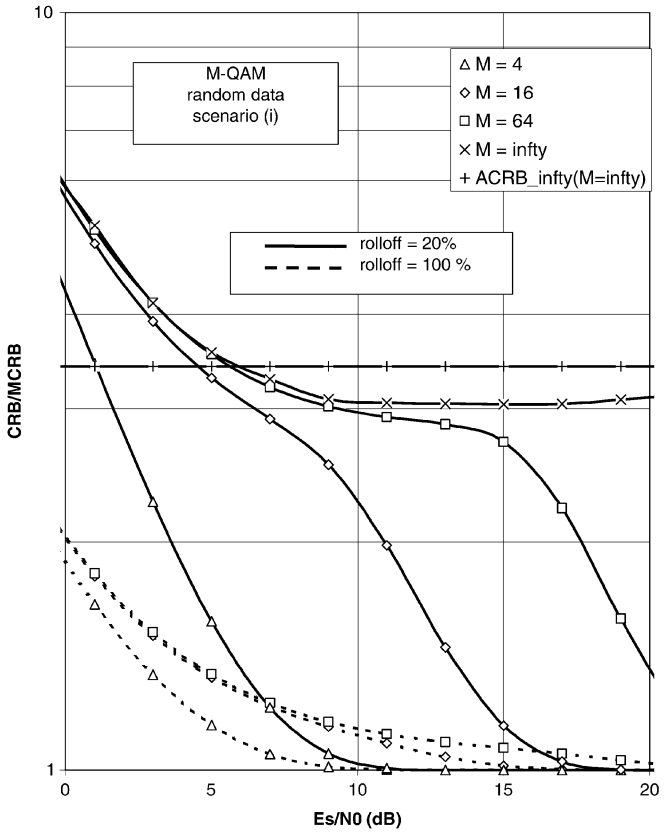

Fig. 4. CRB/MCRB for timing estimation from a noisy linearly modulated signal characterized by a cosine rolloff pulse and random M-QAM symbols.

the ratio $\mathrm{CRB}^{(\mathrm{ii}),\mathrm{kn}}/\mathrm{MCRB}$ depends neither on the shape of the transmit pulse $h(t)$, nor on the constellation.

Also for other constellations and for other values of the excess bandwidth, we have verified that $\mathrm{CRB}^{(\mathrm{i}),\mathrm{ra}}$ and $\mathrm{CRB}^{(\mathrm{ii}),\mathrm{ra}}$ are essentially the same when $L \geq 101$ and E_s/N_0 exceeds 0 dB. Therefore, in the sequel, we restrict our attention to the ratio $\mathrm{CRB}^{(\mathrm{i}),\mathrm{ra}}/\mathrm{MCRB}$.

Figs. 2–4 show the ratio $\mathrm{CRB}^{(\mathrm{i}),\mathrm{ra}}/\mathrm{MCRB}$ with $L = 101$ for M-PAM, M-PSK, and M-QAM, respectively.

Figs. 2–4 indicate that the CRB decreases with increasing rolloff factor, and that this effect is more pronounced at small E_s/N_0 than at large E_s/N_0.

For all three constellations, we observe that for a given E_s/N_0, the ratio CRB/MCRB increases with M, which indicates that for the larger constellations, timing recovery is inherently harder to accomplish (a similar observation holds for carrier synchronization assuming perfect timing recovery [8]–[10]). This effect is more pronounced for a smaller rolloff factor. Figs. 2–4 also show the limiting curve for M approaching infinity (only for 20% rolloff, because for 100% rolloff, the effect of the number (M) of constellation points is much smaller); this situation corresponds to data symbols that are *continuous* random variables, that are uniformly distributed on the unit circle for PSK, in the interval $(-\sqrt{3},\sqrt{3})$ for PAM, and in a $\sqrt{6} \times \sqrt{6}$ square for QAM. It is instructive to consider the high-SNR limit $\mathrm{ACRB}_\infty(M = \infty)$ of the CRB when the number of symbols in the constellation is infinite. Using the method outlined in [4], we obtain

$$\mathrm{ACRB}_\infty(M=\infty) = \begin{cases} \frac{N_0}{2E_sL} \cdot \frac{1}{C_1 - C_2}, & \text{PAM, QAM} \\ \frac{N_0}{2E_sL} \cdot \frac{1}{C_1 - \frac{1}{2}C_2}, & \text{PSK.} \end{cases} \tag{37}$$

Expression (37) indicates that for large E_s/N_0, the CRB in the case of infinite-size constellations does not approach the MCRB (9); according to [4], this is because of the nondiagonal nature of the FIM, related to the joint estimation of the continuous data symbols and the time delay. This behavior is confirmed by the nearly horizontal portion of the curves corresponding to infinite M that occurs at large E_s/N_0 (see Figs. 2–4). Note from (37) that the ratio $\mathrm{ACRB}_\infty\ (M = \infty)/\mathrm{MCRB}$ is larger for PAM and QAM than for PSK; this can also be verified from Figs. 2–4. When $M = \infty, \mathrm{ACRB}_\infty$ is not necessarily a lower bound on the mean-square estimation error for finite E_s/N_0; this can be seen from Figs. 2 and 4, where the nearly horizontal portion of $\mathrm{CRB}\ (M = \infty)/\mathrm{MCRB}$ is below $\mathrm{ACRB}_\infty\ (M = \infty)/\mathrm{MCRB}$.

For finite M, the CRB does converge to the MCRB when E_s/N_0 is sufficiently large. The value of E_s/N_0, at which CRB is close to MCRB, increases by about 6 dB when M doubles (PAM, PSK) or quadruples (QAM). It is outlined in Appendix II that the convergence to the MCRB is mainly determined by the value of $(E_s/N_0)d_{\min}^2$, with $d_{\min}$ denoting the minimum Euclidean distance between the constellation points. For all considered constellations, we have verified that the convergence of

CRB to MCRB occurs at a value of E_s/N_0 that corresponds to an uncoded BER in the order of 10^{-3}.

In the case of transmit pulses $h(t)$ that are time-limited to one symbol interval T, we have $\dot{g}(mT) = 0$ for all m, so that only the first term of (22) contributes. This yields $\mathrm{CRB/MCRB} = 1/A(E_s/N_0)$, which does not depend on the shape of the time-limited transmit pulse. We have verified that the curves corresponding to a rolloff of 100% yield essentially the same result. Hence, the curves for 100% rolloff are representative also for time-limited transmit pulses.

V. Comparison of CRB and Actual Synchronizer Performance

Here we compare the CRB to the mean-square timing errors (MSEs) resulting from a nondata-aided (NDA) and a decision-directed (DD) symbol synchronizer. We assume random data taken from a 4-PSK constellation, a square-root cosine rolloff transmit pulse with a 20% excess bandwidth, and an observation interval of $L = 101$ symbols.

The NDA synchronizer is the well-known Oerder & Meyr (O&M) synchronizer that has been introduced and analyzed in [12]. The O&M synchronizer derives its timing estimate from the Fourier transform, evaluated at $f = 1/T$, of the squared magnitude of the matched-filter output. In contrast to the DD symbol synchronizer described below, the O&M synchronizer performs timing estimation independently of carrier synchronization. The O&M synchronizer performance does not depend on the carrier phase θ, and is only marginally affected by a small carrier frequency offset F (because τ and F are decoupled); therefore, we have determined the MSE assuming $F = 0$.

The DD synchronizer is related to the likelihood function $p(\mathbf{r} \,|\, \mathbf{a}; \theta, F, \tau)$. The synchronizer jointly maximizes over (τ, F, θ) the function $L_{\mathrm{DD}}\,(\tau, F, \theta)$, given by

$$L_{\mathrm{DD}}(\tau, F, \theta) = \sum_{k=-K}^{K} \Re[\hat{a}_k^* e^{-j\theta} x_k(\tau, F)]$$

where $x_k\,(\tau, F)$ is defined in (5), and $\hat{a}_k$ results from applying $e^{-j\theta} x_k\,(\tau, F)$ to the hard-decision device. The maximization of $L_{\mathrm{DD}}\,(\tau, F, \theta)$ is to be carried out iteratively. From a previous estimate $(\hat{\tau}_i, \hat{F}_i, \hat{\theta}_i)$, a refined estimate $(\hat{\tau}_{i+1}, \hat{F}_{i+1}, \hat{\theta}_{i+1})$ is computed, based upon the derivatives of $L_{\mathrm{DD}}\,(\tau, F, \theta)$ with respect to τ, F, and θ, evaluated at $(\hat{\tau}_i, \hat{F}_i, \hat{\theta}_i)$. An initial estimate $\hat{\tau}_0$ is obtained from the O&M synchronizer described above; using $\tau = \hat{\tau}_0$, an initial estimate $(\hat{F}_0, \hat{\theta}_0)$ can be provided by an NDA carrier synchronizer suited to the symbol constellation (examples of such carrier synchronizers can be found in [7], [8], [13], and [14]). As τ is decoupled from (F, θ), the accuracy of the timing estimate is not affected by (small) carrier synchronization errors; therefore, we have determined the MSE, assuming that F and θ are known to the receiver $(F = \theta = 0)$.

Fig. 5 compares the ratios $\mathrm{CRB}^{(\mathrm{i}),\mathrm{ra}}/\mathrm{MCRB}$, $\mathrm{MSE}_{\mathrm{NDA}}/\mathrm{MCRB}$, and $\mathrm{MSE}_{\mathrm{DD}}/\mathrm{MCRB}$, with $\mathrm{MSE}_{\mathrm{NDA}}$ and $\mathrm{MSE}_{\mathrm{DD}}$ denoting the MSEs resulting from the NDA and the DD synchronizer, respectively. We have not displayed $\mathrm{CRB}^{(\mathrm{ii}),\mathrm{ra}}/\mathrm{MCRB}$, because for $L = 101$, it is essentially the same as $\mathrm{CRB}^{(\mathrm{i}),\mathrm{ra}}/\mathrm{MCRB}$. As expected, the CRB is a lower bound on the MSE of the NDA and DD symbol synchronizers. For large SNR (say, $E_s/N_0 > 10$ dB), $\mathrm{MSE}_{\mathrm{DD}}$ is very close to the MCRB, which indicates that in this operating region the synchronizer performance is not affected by the decision errors. Synchronizer performance is essentially the same as for *a priori* known data symbols. When E_s/N_0 decreases below 10 dB, decision errors occur more frequently, and therefore, $\mathrm{MSE}_{\mathrm{DD}}$ gets larger than the MCRB. However, when E_s/N_0 is between 5–10 dB, $\mathrm{MSE}_{\mathrm{DD}}$ is close to the true CRB, in spite of the increased number of decision errors. For $E_s/N_0 < 5$ dB, the decision errors are too frequent, and $\mathrm{MSE}_{\mathrm{DD}}$ is larger than the CRB. Hence, the DD synchronizer is close to optimum for moderate and large SNR (i.e., $E_s/N_0 > 5$ dB). The NDA symbol synchronizer shows the opposite behavior: this synchronizer is close to optimum for (very) small SNR, and the deviation of $\mathrm{MSE}_{\mathrm{NDA}}$ from the CRB increases with increasing SNR.

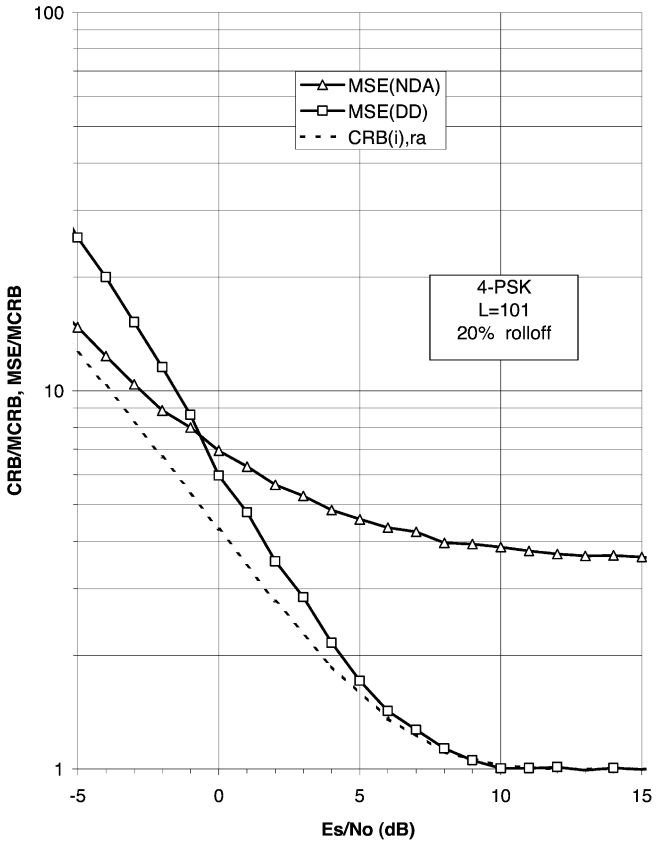

Fig. 5. Comparison of the CRB to the MSE resulting from an NDA and a DD symbol synchronizer.

VI. Conclusions and Remarks

We have derived the CRB related to timing estimation from a noisy linearly modulated signal with arbitrary bandlimited square-root Nyquist transmit pulse. We have handled both random data and *a priori* known training symbols. Two different scenarios were considered: timing estimation jointly with carrier phase and carrier frequency [Scenario (i)]; and timing estimation jointly with the carrier frequency but irrespective of the carrier phase [Scenario (ii)].

The numerical evaluation of the CRBs requires the Monte Carlo evaluation of a few statistical expectations, and for Scenario (ii) also, numerical integration over the unknown carrier phase θ is needed. These averages and numerical integration depend on E_s/N_0 and on the number of symbols in the constellation (and, for Scenario (ii), also on the transmitted sequence length), but not on the pulse shape. The effect of the pulse shape is analytically accounted for.

We have shown analytically that the time delay is decoupled from the carrier phase and frequency in Scenario (i), and from the carrier frequency in Scenario (ii). This implies that the CRB for timing estimation is not affected by whether the decoupled parameters are *a priori* known or estimated jointly with the timing.

Further, we have investigated the dependence of the CRB on E_s/N_0, the pulse shape, the constellation, and the length of the observation interval. We have shown that both scenarios yield a CRB for timing estimation that for moderate and large observation intervals is nearly the same as the CRB for timing estimation in the case of perfect carrier recovery. In the case of a known training sequence, this CRB essentially coincides with the MCRB. In the case of random data, the CRB is very close to the MCRB, when E_s/N_0 is such that the BER for uncoded transmission is less than about 10^{-3}.

The evaluated CRBs were compared to the MSE estimation resulting from existing timing synchronizers. At moderate and high SNR, the DD estimator performs close to the CRB and provides a large improvement over the NDA timing estimator. At (very) low SNR, the NDA synchronizer outperforms the DD synchronizer and converges to the CRB.

We have verified (simulation results not reported here) that when transmitting *coded* 4-PSK symbols, the MSEs of the NDA and DD synchronizer remain essentially the same as for uncoded transmission (with E_s/N_0 denoting the energy per coded symbol, and the DD synchronizer making use of hard symbol-by-symbol decisions about the coded symbols). This indicates that in the case of coded transmission, the CRB for uncoded data symbols can be interpreted as a lower bound on the MSE, resulting from a synchronizer that does not exploit the encoding rule. In the case of *carrier phase* estimation from coded symbols, the CRB corresponding to the normal operating SNR of the code has been shown to be very close to the MCRB [15]–[17]. Hence, the ratio $\mathrm{CRB}_{\mathrm{uncoded}}/\mathrm{MCRB}$ is an indication about how much the synchronizer performance could be improved by making clever use of the code properties in the phase estimation process. Moreover, "code-aware" carrier synchronizers performing close to the MCRB have been presented in [18]–[20]. The extension to timing recovery of these results, pertaining to carrier synchronization from coded signals, is a topic of further research.

Appendix I

Denoting $\mathbf{u}^T = (u_1, u_2, u_3) = (\tau, F, \theta)$, we easily obtain

$$E_{\mathbf{r}\,|\,\mathbf{a}}\left[\frac{\partial^2 \ln(p(r|\mathbf{a},\theta,F,\tau)}{\partial u_k \partial u_\ell}\right] = \Re\left[\sum_{m,n=-K}^{K} a_m^* a_n M_{k,\ell}(m,n)\right] \quad \text{(A1.1)}$$

where

$$M_{k,\ell}(m,n) = \frac{2E_s}{N_0}\int Q_n(t;\theta,F,\tau)\frac{\partial^2 Q_m^*(t;\theta,F,\tau)}{\partial u_k \partial u_\ell}\,dt$$
$$Q_n(t;\theta,F,\tau) = h(t-nT-\tau)\exp(j(2\pi Ft+\theta).$$

In the case of Scenario (i) with *random* data symbols, the elements of the 3×3 MFIM are obtained by averaging (A.1) over the data symbols. This yields

$$(J_M)_{k,\ell} = \Re\left[\sum_{m=-K}^{K} M_{k,\ell}(m,m)\right] \quad \text{for } k,\ell = 1,2,3. \quad \text{(A1.2)}$$

In the case of Scenario (ii) with *random* data, the elements of the 2×2 MFIM are obtained by averaging (A1.1) over the data symbols and the carrier phase for $k,\ell = 1,2$. However, it is easily verified that $M_{k,\ell}(m,n)$ does not depend on θ, so that the MFIM for Scenario (ii) is a submatrix of the MFIM for Scenario (i). Assuming real-valued transmit pulses, it has been shown in [3] that $(J_M)_{1,2} = (J_M)_{1,3} = 0$, so that for both scenarios, the MCRB corresponding to random data equals $1/(J_M)_{1,1}$, which yields (8).

In the case of Scenario (i) with known training symbols, the elements of the MFIM are given by (A1.1) for $k,\ell = 1,2,3$. The MIFM related to Scenario (ii) is a 2×2 submatrix of the MFIM for Scenario (i). For increasing L, the elements (A1.1) of the MFIM converge to (A1.2), which are the elements of the MFIM in the case of random data. Hence, the resulting MCRB is given by (8) as well.

Appendix II

We consider both the MCRB and the CRB for timing estimation, resulting from the joint estimation of (τ, F, θ), in the case of a random data sequence $\mathbf{a} = \{a_k\}$. As τ is decoupled from (F,θ), the CRB is the same as for estimating τ assuming (F,θ) is known. In this case, the MCRB from (2) is computed from the derivative of the joint LLF of $\mathbf{a}$ and τ, with respect to τ given by

$$\frac{d\ln p(\mathbf{r}\,|\,\mathbf{a};\tau)}{d\tau} = \frac{2E_s}{N_0}\sum_{k=-K}^{K}\Re\left[a_k^*\frac{dx_k}{d\tau}\right]. \quad \text{(A.2.1)}$$

The resulting MCRB equals (8). At the same time, the CRB from (1) is determined by the derivative of the (marginal) LLF of τ, which can be manipulated into the following form:

$$\frac{d\ln p(\mathbf{r};\tau)}{d\tau} = \frac{2E_s}{N_0}\sum_{k=-K}^{K}\left(\frac{\sum_{i=0}^{M-1}\Re\left[\alpha_i^*\frac{dx_k}{d\tau}\right]R(k,i)}{\sum_{i=0}^{M-1}R(k,i)}\right) \quad \text{(A.2.2)}$$

with $\{\alpha_0,\alpha_1,\ldots,\alpha_{M-1}\}$ denoting the set of constellation points, and

$$R(k,i) = \exp\left\{-\frac{E_s}{N_0}[|a_k-\alpha_i|^2 + 2\Re(n_k^*(a_k-\alpha_i))]\right\}. \quad \text{(A.2.3)}$$

In (A.2.3), a_k represents the kth data symbol transmitted, and n_k is a zero-mean complex Gaussian noise term with indepen-

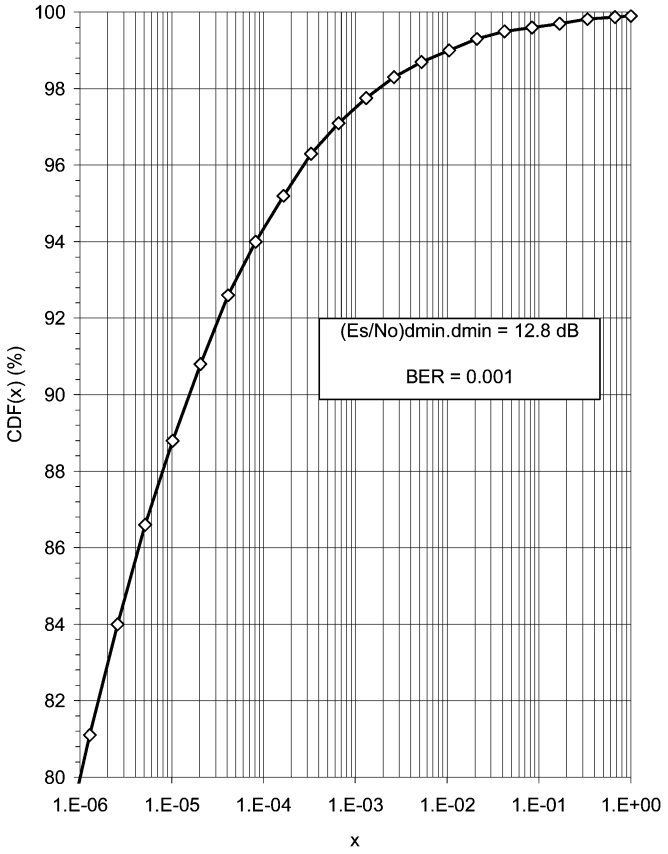

Fig. 6. Cumulative distribution function of $R(k,i)$ $(\mathrm{CDF}(x) = P[R(k,i) \le x])$ as a function of x.

dent real and imaginary parts, each having a variance equal to $N_0/2E_s$. Note that $R(k,i) = 1$ when $\alpha_i = a_k$. It is easily verified that, for given a_k, the quantity $R(k,i)$ is lognormally distributed with median value[1] equal to

$$\exp(E[\ln R(k,i)]) = \exp\left(-\frac{E_s}{N_0} d^2(k,i)\right) \qquad \text{(A.2.4)}$$

where $d(k,i) = |a_k - \alpha_i|$. It follows from (A.2.4) that the quantities $R(k,i)$ with $\alpha_i \neq a_k$ are likely to be much smaller than one when $(E_s/N_0)\, d^2\ (k,i)$ is large. In this case, both the numerator and the denominator of the kth term in (A.2.2) are, with high probability, strongly dominated by the term with $\alpha_i = a_k$ (for which $R(k,i) = 1$), so that the right-hand side of (A.2.2) is well approximated by the right-hand side of (A.2.1). This indicates that $\mathrm{CRB}^{(\mathrm{i}),\mathrm{ra}}$ converges to MCRB with increasing E_s/N_0.

Let us verify that the quantities $R(k,i)$ with $\alpha_i \neq a_k$ are indeed likely to be much smaller than one when E_s/N_0 is such that the BER is about 10^{-3}. For the various constellations considered, a BER in the order of 10^{-3} corresponds to $(E_s/N_0)\ d^2_{\min} \cong 19.2$ (or, in decibels, $10\log(E_s/N_0) + 20\log\ (d_{\min}) \cong 12.8$ dB), where $d_{\min}$ denotes the minimum Euclidean distance between the constellation points. At high E_s/N_0, the quantities $R(k,i)$ with $|a_k - \alpha_i| = d_{\min}$ are most likely to be the second largest of all $R(k,i)$. The cumulative distribution function $\mathrm{CDF}(x) = P[R(k,i) \le x]$ corresponding to $|a_k - \alpha_i| = d_{\min}$ is plotted in Fig. 6 as a function of x, for $(E_s/N_0)\ d^2_{\min} = 12.8$ dB (or $\mathrm{BER} \cong 10^{-3}$). We observe that the considered $R(k,i)$ are less than 10^{-3} (10^{-2}) in about 97.5% (99%) of all cases, which indicates that they can be neglected, as compared with $R(k,i) = 1$.

[1]The lognormal distribution is highly skewed to the right (asymmetrical with right tail longer then left). The median is less affected by extreme scores than the mean and is, therefore, a better measure of central tendency for such an extremely skewed distribution.

REFERENCES

[1] H. L. Van Trees, *Detection, Estimation and Modulation Theory*. New York: Wiley, 1968.

[2] A. N. D'Andrea, U. Mengali, and R. Reggiannini, "The modified Cramer–Rao bound and its applications to synchronization problems," *IEEE Trans. Commun.*, vol. 24, pp. 1391–1399, Feb.-Apr. 1994.

[3] F. Gini, R. Reggiannini, and U. Mengali, "The modified Cramer–Rao bound in vector parameter estimation," *IEEE Trans. Commun.*, vol. 46, pp. 52–60, Jan. 1998.

[4] M. Moeneclaey, "On the true and the modified Cramer–Rao bounds for the estimation of a scalar parameter in the presence of nuisance parameters," *IEEE Trans. Commun.*, vol. 46, pp. 1536–1544, Nov. 1998.

[5] H. Steendam and M. Moeneclaey, "Low-SNR limit of the Cramer–Rao bound for estimating the time delay of a PAM, PSK, or QAM waveform," *IEEE Commun. Lett.*, vol. 5, pp. 31–33, Jan. 2001.

[6] ——, "Low-SNR limit of the Cramer–Rao bound for estimating the carrier phase and frequency of a PAM, PSK, or QAM waveform," *IEEE Commun. Lett.*, vol. 5, pp. 215–217, May 2001.

[7] W. G. Cowley, "Phase and frequency estimation for PSK packets: Bounds and algorithms," *IEEE Trans. Commun.*, vol. 44, pp. 26–28, Jan. 1996.

[8] F. Rice, B. Cowley, B. Moran, and M. Rice, "Cramer–Rao lower bounds for QAM phase and frequency estimation," *IEEE Trans. Commun.*, vol. 49, pp. 1582–1591, Sept. 2001.

[9] N. Noels, H. Steendam, and M. Moeneclaey, "The true Cramer–Rao bound for phase-independent carrier frequency estimation from a PSK signal," in *Proc. IEEE GLOBECOM*, Taipei, Taiwan, Nov. 2002, pp. 1137–1141.

[10] ——, "The impact of the observation model on the Cramer–Rao bound for carrier and frequency synchronization," in *Proc. IEEE Int. Conf. Communications*, Anchorage, AK, May 2003, pp. 2562–2566.

[11] ——, "The true Cramer–Rao bound for edtimating the time delay of a linearly modulated waveform," in *Proc. IEEE Int. Conf. Communications*, New York, NY, Apr./May 2002, pp. 1476–1479.

[12] M. Oerder and H. Meyr, "Digital filter and square timing recovery," *IEEE Trans. Commun.*, vol. COM-36, pp. 605–612, May 1988.

[13] A. J. Viterbi and A. M. Viterbi, "Nonlinear estimation of PSK-modulated carrier phase with application to burst digital transmission," *IEEE Trans. Inform. Theory*, vol. IT-29, pp. 543–551, July 1983.

[14] H. Meyr, M. Moeneclaey, and S. A. Fechtel, *Digital Communication Receivers—Synchronization, Channel Estimation, and Signal Processing*. New York: Wiley, 1998.

[15] N. Noels, H. Steendam, and M. Moeneclaey, "The true Cramer–Rao bound for estimating the carrier phase of a convolutionally encoded signal," in *Proc. IEEE SVCT*, 2002, pp. 9–14.

[16] ——, The true Cramer–Rao bound for carrier and symbol synchronization. presented at *EUSIPCO*. [CD-ROM]Paper 890

[17] ——, "The Cramer–Rao bound for phase estimation from coded linearly modulated signals," *IEEE Commun. Lett.*, vol. 7, pp. 207–209, May 2003.

[18] N. Noels *et al.*, "Turbo synchronization: An EM algorithm interpretation," in *Proc. IEEE Int. Conf. Communications*, Anchorage, AK, May 2003, pp. 2933–2937.

[19] H. Steendam, N. Noels, and M. Moeneclaey, "Iterative carrier phase synchronization for low-density parity-check coded systems," in *Proc. IEEE Int. Conf. Communications*, Anchorage, AK, May 2003, pp. 3120–3124.

[20] V. Lottici and M. Luise, "Carrier phase recovery for turbo-coded linear modulations," in *Proc. IEEE Int. Conf. Communications*, New York, NY, Apr./May 2002, pp. 1541–1545.

Nele Noels (S'02) received the diploma of electrical engineering in 2001 from Ghent University, Gent, Belgium, where she is currently working toward the Ph.D. degree in the Department of Telecommunications and Information Processing.

Her main research interests are in carrier and symbol synchronization. She is the author of several papers in international journals and conference proceedings.

Henk Wymeersch (S'02) received the diploma of computer science engineer in 2001 from Ghent University, Gent, Belgium, where he is currently working toward the Ph.D. degree in the Department of Telecommunications and Information Processing.

His main research interests include channel coding and synchronization.

Heidi Steendam (M'00) received the Diploma and the Ph.D. degree, both in electrical engineering, from Ghent University, Gent, Belgium, in 1995 and 2000, respectively.

She is currently a Professor in the Department of Telecommunications and Information Processing, Ghent University. Her main research interests are in statistical communication theory, carrier and symbol synchronization, bandwidth-efficient modulation and coding, spread spectrum (multicarrier spread spectrum), satellite and mobile communication. She is the author of more than 50 scientific papers in international journals and conference proceedings.

Marc Moeneclaey (M'93–SM'99–F'02) received the Diploma and the Ph.D. degree, both in electrical engineering, from Ghent University, Gent, Belgium, in 1978 and 1983, respectively.

He is currently a Professor in the Department of Telecommunications and Information Processing, Ghent University. His main research interests are in statistical communication theory, carrier and symbol synchronization, bandwidth-efficient modulation and coding, spread spectrum, satellite and mobile communication. He is the author of more than 200 scientific papers in international journals and conference proceedings. Together with H. Meyr (RWTH Aachen) and S. Fechtel (Siemens AG), he is a co-author of the book *Digital Communication Receivers—Synchronization, Channel Estimation, and Signal Processing* (New York: Wiley, 1998).

Between 1992–1994, Dr. Moeneclaey served as Editor for Synchronization for the IEEE TRANSACTIONS ON COMMUNICATIONS.